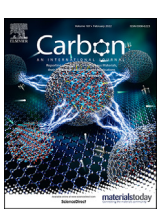
FISEVIER

Contents lists available at ScienceDirect

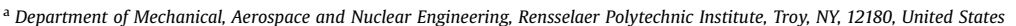
Carbon

journal homepage: www.elsevier.com/locate/carbon



Reversing fatigue in carbon-fiber reinforced vitrimer composites

Mithil Kamble ^{a, 1}, Aniruddh Vashisth ^{b, 1}, Hongkun Yang ^{c, 1}, Sikharin Pranompont ^a, Catalin R. Picu ^{a, ***}, Dong Wang ^{c, **}, Nikhil Koratkar ^{a, d, *}



^b Department of Mechanical Engineering, University of Washington, Seattle, WA, 98195, United States

ARTICLE INFO

Article history:
Received 9 September 2021
Received in revised form
27 October 2021
Accepted 29 October 2021
Available online 2 November 2021

Keywords: Vitrimers Fatigue Healing Carbon-fiber composites

ABSTRACT

Despite decades of research, fatigue remains the primary culprit for catastrophic failure in carbon-fiber reinforced polymeric (CFRP) composites. Existing approaches to combat fatigue are usually based on nano-scale additives that slow the growth of cracks in the polymer. While this prolongs fatigue-life, it cannot avert eventual failure since crack growth is being slowed and not reversed. Other approaches have explored self-healing polymers that release a curing agent to repair local damage. However, this approach also fails to tackle fatigue, since once the curing agent is released, it gets consumed and cannot be re-used. To addresses the irreversibility of fatigue, we report here a vitrimeric system, for which reversal of fatigue damage can be achieved repeatedly, by heating the material to above its topology freezing transition temperature. This enables intermittent healing of fatigue-induced damage, as it accumulates in the vitrimer matrix. Using this approach, we show that fatigue failure in vitrimers and in carbon-fiber reinforced vitrimers (vCFRP) can be postponed indefinitely. Such vCFRPs could open the door to future materials, in which natural aging and fatigue processes can be periodically reversed, so as to guarantee safe and reliable long-term operation.

© 2021 Elsevier Ltd. All rights reserved.

1. Introduction

Carbon-fiber reinforced polymer composites (CFRP) are becoming ubiquitous in high performance structural applications. They are being extensively used in the aerospace, marine, automotive, sports and renewable energy industries. While the bulk of the load is carried by carbon fibers in CFRP, lightweight thermoset polymers like epoxy provide structural integrity as the matrix. This enables CFRP to exhibit specific modulus and strength that is superior to most metals. However, CFRP are susceptible to fatigue failure [1] which typically initiates in the matrix at the location of heterogeneities or flaws [2]. Thus, the same polymeric matrix which enables CFRP to achieve high specific modulus and strength

E-mail addresses: picuc@rpi.edu (C.R. Picu), dwang@mail.buct.edu.cn (D. Wang), koratn@rpi.edu (N. Koratkar).

also impedes its fatigue performance, which poses a unique design challenge. CFRP are expected to represent a ~\$31 Billion global market by 2024 [3], driven by the soaring demand for lightweight and high-performance structural materials. However, a major cost associated with CFRP are the structural health monitoring (SHM) systems [4] that are required to detect fatigue damage. These SHM systems are projected to cost ~\$5.5 Billion by 2024 [5]. Hence, developing fatigue resistant composites is a pressing need for the CFRP community and considerable research efforts are directed towards this goal [6–8].

Fatigue failure in polymeric matrices originates from incipient flaws and its origin is best understood from the network perspective. Thermoset polymers are a network of molecular chains which are densely cross-linked during the curing process to form a rigid structure. These cross-links impart desirable properties such as high strength, stiffness, and thermal stability [9]. However, these cross-links can irreversibly rupture during the lifecycle of a component, and this triggers crack growth processes which results in eventual failure. A popular approach to prolong the fatigue life of polymers has been by incorporating nano-additives in them. Nano-additives interact with incipient cracks and significantly retard

^c State Key Laboratory of Organic–Inorganic Composites, Beijing University of Chemical Technology, Beijing, 100029, China

d Department of Materials Science and Engineering, Rensselaer Polytechnic Institute, Troy, NY, 12180, United States

^{*} Corresponding author.

^{**} Corresponding author.

^{***} Corresponding author. Department of Mechanical, Aerospace and Nuclear Engineering, Rensselaer Polytechnic Institute, Troy, NY, 12180, United States.

¹ Equal Contribution.

crack growth in nanocomposites [10]. Various nano-additives like nano-silica, graphene and carbon nanotubes have been demonstrated to improve the fracture and fatigue performance of polymers [11-13]. However, the nanocomposites approach is fundamentally limited by the "irreversibility" of the damage induced in thermoset polymers. Once a crack is initiated in the matrix, it would eventually reach critical crack growth rate which results in catastrophic failure. Nano-additives slow crack propagation and prolong fatigue life, but they cannot avert eventual failure. To mitigate the irreversibility of damage, self-healing polymers which contain curing agent filled micropores have been explored [14,15]. Micropores can be ruptured by an approaching crack, which releases curing agent that repairs the local damage by the sealing of microcracks. However, this approach cannot prevent eventual fatigue failure, as once initial rupture of pores is over, the curing agent gets consumed and the next microcracks accumulate the damage irreversibly.

To address the irreversibility of fatigue damage, the molecular network structure of polymers must be considered. Permanent cross-links in fully cured thermoset networks impart desirable properties while making them predisposed to irreversible damage. Thermoplastics, which are molecular networks without cross-links, can be repaired after structural damage by reprocessing them above their melting temperatures. However, since they are not crosslinked, they lack the strength, stiffness, thermal and chemical stability required in high performance applications [16]. Hence, it is evident that an ideal polymer for CFRP would be a molecular network with reversible cross-links which would be as strong as thermosets, while also possessing abilities to reverse the damage like thermoplastics. Leibler et al. achieved a breakthrough in this direction when they proposed an epoxy-based associative network which undergoes reversible cross-linking reaction at elevated temperatures [17]. Such networks can be conveniently manufactured by reaction of conventional epoxy with a carboxylic acid and a suitable catalyst. These materials are termed vitrimers since their viscosity behavior approaching the glass transition temperature (T_g) follows an Arrhenius law and is analogous to vitreous silica. Vitrimers are characterized by a topology freezing transition temperature (T_v), above which the reversible crosslinking reaction can be achieved at higher rates, enabling self-healing capabilities [18,19].

While there has been considerable research on vitrimers [17-23] their fatigue behavior remains entirely unexplored. Moreover, their fatigue performance within CFRP systems has not been reported. In this study, we have developed a vitrimeric matrix and created vitrimeric CFRP (vCFRP), for which reversal of fatigue damage can be achieved repeatedly, by heating the sample to above T_v. Our results indicate that by this approach, fatigue failure in vCFRP can be potentially postponed indefinitely by periodically healing the fatigue damage, as it accumulates in the vitrimer matrix. Such a healing strategy successfully addresses the irreversible nature of fatigue and achieves repeated reversal of fatigue-induced damage in vitrimers and in vCFRP systems. The initial part of this letter deals with experimental and simulation development of healing in the pure vitrimer (i.e. without carbon fibers) and the last part presents its application to the vCFRP system. This sequence allows us to first study and understand fatigue reversal in the pure vitrimer matrix, before extending the fatigue healing concept to the full vCFRP

2. Materials and methods

2.1. Molecular dynamics

1:1 M ratio of Diglycidyl ether of bisphenol-A (DGEB-A) and adipic acid (Fig. S1) was used for constructing the virtual system.

CHNO-2017_weak force field modified by Vashisth et al. [24] was used for the ReaxFF simulations including minimization, equilibration and accelerated crosslinking simulations. This force field was selected as it contains the parameters related to hydrocarbons and the parameters for C-O, C-N, and N-H bond terms, angle terms of oxygen and nitrogen atoms, and the hydrogen bonding parameters of nitrogen were optimized to improve their reproduction of epoxide/amine coupling reactions. Accelerated ReaxFF simulations were carried out in NVT conditions, and extra energy (E_{rest} – see Supporting Information) was provided to the reactive sites over 10,000 iterations of 0.25 femtosecond to obtain successful crosslinking using the determined force constants. Annealing of the virtual polymer was performed by elevating the temperature of the system from 300 K to 600 K and then cooling back to 300 K; this was done repeatedly until consecutive annealing resulted in similar densities.

2.2. Materials

All chemical products were commercially available and were used as received without further purification. High strength aerospace grade woven carbon fabrics (Toho-Tenax Japan, HTS40-3K, basis weight of 200 g m $^{-2}$) were used to fabricate the vCFRP. DGEBA (DER 332, molecular weight (M.W.) = 340.14 g mol $^{-1}$) and adipic acid (99%, M.W. = 146.14 g mol $^{-1}$) were purchased from Sigma-Aldrich. 1,5,7-triazabicyclo [4,4,0] dec-5-ene (TBD, 98%, M.W. = 139.2 g mol $^{-1}$) was obtained from J&K.

2.3. Preparation of epoxy Vitrimer and vCFRP

To synthesize the vitrimer, stoichiometric amounts of DGEBA and adipic acid were first mixed in a vial and heated to 160 °C with stirring. Then, the catalyst TBD (2.5 mol% to the COOH) was added in the mixture. The precursors were stirred until homogeneous, and then the viscous solution was rapidly poured into PTFE molds and cured in a hot press at 160 °C and 10 MPa for 6 hours. The resulting dogbone specimen of overall dimension $20 \times 50 \text{ mm}^2$ was used for the mechanical characterization of vitrimers. To synthesize the vCFRP prepreg, vitrimer precursors were stirred until homogeneous and then the viscous solution was rapidly poured into onelayer carbon-fiber lamina and pressed under 2 MPa pressure for 15 min at 160 °C. To prepare vCFRP laminates, 8 prepreg sheets were stacked and cured at 160 °C for 6 hours under 10 MPa pressure. The as prepared vCFRP laminates Fig. S10 have an average thickness of ~2.4 mm. Rectangular specimen of dimension $10 \times 75 \text{ mm}^2$ were cut out for the vCFRP characterization.

2.4. Dilatometry experiment

Dilatometry also carried out using a dynamic mechanical analyzer (TA DMA 850) in controlled force tension mode by applying stress of ~100 kPa and heated from $-20\,^{\circ}\text{C}$ to $230\,^{\circ}\text{C}$ at a heating rate of $2.5\,^{\circ}\text{C}$ min⁻¹. The samples were subjected to preload of 0.01 N and equilibrated at the starting temperature for 5 min. The sample dimensions were $15\times5\times0.9\,\text{mm}^3$.

2.5. Differential scanning calorimetry (DSC)

These experiments were performed on a TA DSC 25 equipped with a RCS90 refrigerated cooling system. Samples were heated from room temperature to 180 °C under a nitrogen atmosphere and maintained at this temperature for 3 min to erase thermal history. The samples were then cooled to 0 °C and re-heated to ~180 °C. The heating and cooling rates were 10 °C min $^{-1}$. Glass transition temperatures ($T_{\rm g}$) were recorded during the second heating ramp.

2.6. Stress relaxation analysis (SRA)

These experiments were performed on a TA DMA 850 in strain control mode with sample dimension of 15 \times 5 \times 0.9 mm³. To ensure good contact of the sample with the geometries, a preload force of 0.001 N was applied. The samples were first equilibrated at specified temperature for 5 min and then were subjected to 1% strain in the linear viscoelastic range. The stress was monitored over time while maintaining the constant strain of 1%. The stress relaxation time τ was determined until the stress was relaxed to at least 1/E of its initial value.

2.7. Mechanical testing

Mechanical testing was performed on an MTS 858 servo hydraulic testing machine. The tensile loading test was performed according to ASTM D638 with strain rate of 0.05 ε sec⁻¹. The tests were also carried out at rates 10 times higher and lower than the initial test to assess the rate sensitivity of the material. Tensile fatigue test was performed in displacement control in accordance with ASTM E638 at the frequency of 1 Hz and maximum strain of 0.005. The healing behavior in vitrimer was assessed by repeating the tensile fatigue test on a pristine sample with intermittent heating at 80 °C for 1 hour and cooling to ambient. vCFRP specimen were loaded in three point bending setup in accordance with ASTM D790 with displacement rate of 1 mm sec^{-1} to get strength σ_{ii} . The flexural fatigue test was carried out in accordance with ASTM D774 in force control mode at the frequency of 1 Hz and peak stress of σ_{11} 2. Healing experiment was carried out by repeating the fatigue test with intermittent healing at 150 °C for 1 hour and cooling to ambient.

3. Simulation of healing behavior

3.1. Molecular dynamics for vitrimers

The vitrimer chemistry and the damage healing process has

been simulated in Fig. 1. Various methods have been proposed to simulate cross-linking of epoxy networks through molecular dynamics (MD). However, earlier methods focus on using the "cut-off" distance approach, where the probability of the reactive sites to react is dependent on their relative distance without considering the reaction pathway [22,23]. In this study, we employ a recently developed and more realistic method [24.25] of crosslinking epoxy polymers, and simulating the healing process within the framework of reactive molecular dynamics (ReaxFF) that uses the "bond boost" approach [26,27] to speed up the MD simulations. In this approach called Accelerated ReaxFF, in addition to the cut-off distance criterion, the reactive sites in the reactants are provided with boost energy — equivalent or slightly larger than the energy reaction barrier — to overcome the cross-linking process barrier and form desired products. This enables cross-linking simulations at realistic low temperatures, which helps mimicking chemical reactions. This approach avoids unwanted high-temperature side reactions, while still allowing for rejection of high-barrier events. Note that catalysts in epoxy-acid vitrimers facilitate controlled exchange reaction rates. In the current simulations, since only the polymerization and the transesterification (healing) reactions are boosted, we did not model the catalyst.

The vitrimer specimen for virtual characterization was fabricated using bisphenol-A and adipic acid in 1:1 M ratio (Fig. S1). In this study, we utilize an Accelerated ReaxFF algorithm, for which two sets of values need to be determined, namely the distance range between the reactive sites and the force constants that result in correct amount of extra energy or bond boost energy (Eq. (2), Supporting Information). The force parameters for Accelerated ReaxFF (i.e. F_1 , F_2 and R_{12} , Supporting Information) were determined for four sets of atom combinations as shown in Fig. S2; this was done through an iterative procedure that resulted in the least amount of input energy. A detailed description of the crosslinking methodology can be found in References 21-22. Fig. 1a shows the reaction coordinates of a single bisphenol-A and adipic acid reaction, where the initial state, transition state, and the final structure are successfully captured by our simulations.

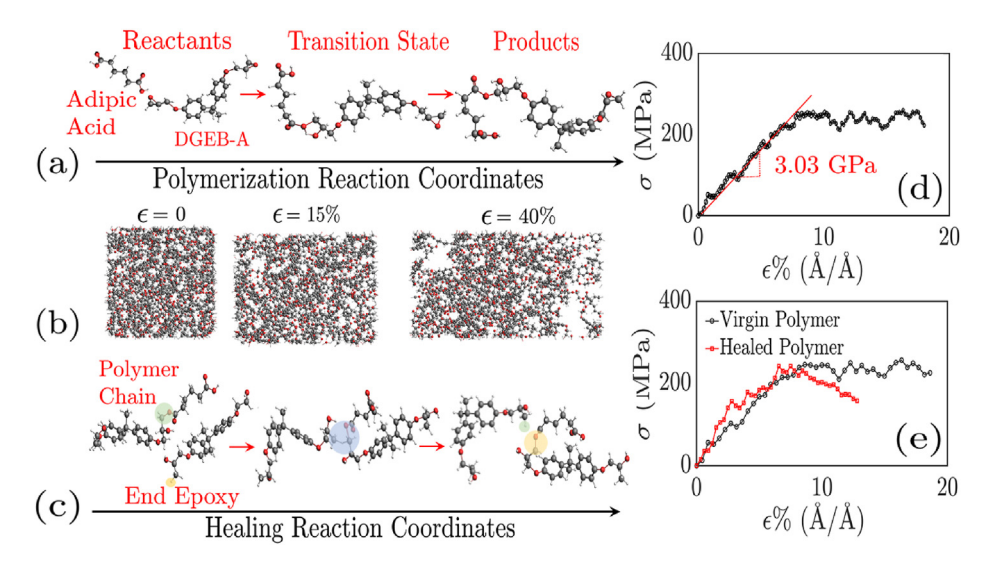


Fig. 1. Simulating the vitrimer and its healing using molecular dynamics. (a) Reaction coordinates for vitrimer polymerization with DGEB-A and adipic acid as initial reactants. A polymerized system was generated by using Accelerated ReaxFF algorithm, and annealed to remove any local heterogeneities. (b) The polymerized system was virtually tested in tension at a strain rate of $^{-10^8}$ (s $^{-1}$ — the snapshots at 0, 15%, and 40% strain are indicated in the figure. (c) Reaction coordinates for the healing reaction; a polymer chain with DGEB-A/adipic acid goes though transesterification reaction, where the adipic acid switches from one epoxy molecule to the other. (d) The Young's modulus of the virgin vitrimer was calculated by fitting linear regression between strain values of 0–7.5% from the stress-strain curves, and found to be 3.03 GPa in the x-direction. The modulus averaged over the x, y and z directions was $^{-2.6}$ ± 0.7 GPa. (e) The failed specimen was healed using the Accelerated ReaxFF simulations and tensile tested again — the healed specimen retains its modulus and strength along the x-direction. (A colour version of this figure can be viewed online.)

The final virtual polymer consisted of ~4000 atoms, this system was equilibrated and then annealed to remove local heterogeneities. The final density of the vitrimer was calculated to be $1.215\pm0.006\,\mathrm{g\,cm^{-3}}$. Similar densities are observed after annealing cycles 2 and 3 in Fig. S3a. The molecular configuration attained at the end of annealing cycle 3 (Fig. S3b) is used as the virtual specimen for all further MD simulations. Glass transition temperature (Tg) of the vitrimer was calculated by running successive NPT and NVT simulations. Fig. S4 shows the average density calculated over each NPT simulation carried out for 2.5 ps at 0.101 MPa and 500 fs damping constant with subsequent temperature ramp at 4 K ps $^{-1}$. The simulated Tg was calculated to be ~42.8 °C by computing the inflection in the density — temperature plot. This result shows excellent quantitative agreement with our experimental results (see Fig. 2a) described later in this letter.

3.2. Mechanical characterization

Next, we used MD simulations to predict the vitrimer's tensile modulus and strength. Since it is challenging to simulate experimental strain rates for calculating the modulus, we resorted to high strain rate testing [1]. A strain rate of $1 \times 10^8 \, \epsilon \, \text{sec}^{-1}$, was used to simulate the tensile mechanical test of the vitrimer. The Young's modulus in the simulations is calculated (Fig. 1d) by fitting a linear regression over the stress-strain curves up to ~7.5% strain. The modulus (averaged in x, y, z directions) was predicted to be \sim 2.6 \pm 0.7 GPa. Virtual specimens experience failure due to changes in non-bonded interactions and bond-rupturing failures. The fractured vitrimer specimen after the simulated tensile test (see Fig. 1b) was next "healed" using the bond boost approach using an NVT ensemble at 80 °C (353 K) and 0.101 MPa. For the vitrimer chemistry that we use, healing is achieved by the transesterification reaction that results in topological rearrangements that preserve the network integrity. Since these reactions have slow kinetics, they cannot be captured by conventional MD. In the Accelerated ReaxFF method, the activation energy for these reactions is provided

through bond boost, enabling them to be successfully modeled. The bond boost parameters that we employed are indicated in Fig. S5 in the supporting information.

3.3. Vitrimer healing mechanism

The healing mechanism seen in the bisphenol-A/adipic acid system is simulated in Fig. 1c. Briefly, a polymer chain with bisphenol-A/adipic acid undergoes a transesterification exchange reaction leading to the acid group exchanging the bisphenol-A polymer chain. The tagged atoms (Fig. S5) were used to provide boost to simulate the transesterification healing mechanism. The healed polymer is annealed to ensure that any local heterogeneities developed during the testing are removed. After annealing, the vitrimer is tested again in tension to obtain the stress-strain relationship. Fig. 1e shows the stress-strain curve for specimens tested along the x-direction at $1\times 10^8~{\rm s}^{-1}$ strain rate, before and after the healing. Interestingly, the sample retains both its intrinsic modulus as well as strength after the healing exercise, which indicates that damage accumulation can be successfully reversed through topological rearrangement of the polymeric network in such systems.

4. Characterization of vitrimers

4.1. Thermomechanical analysis

Vitrimers with the chemistry shown in Fig. 1 were synthesized experimentally. We used diglycidyl ether of bisphenol A (DGEB-A) as monomer with adipic acid as cross-linker, in the presence of triazabicyclodecene as catalyst (Materials and methods). The asproduced vitrimer samples were subjected to thermo-mechanical characterization to establish their characteristic temperatures. Dilatometric analysis (Fig. 2a) indicates onset of material flow at ~44.3 $^{\circ}$ C, which indicates the Tg of the vitrimer. Beyond Tg another plateau is observed where the flow is controlled by the transesterification reaction kinetics [17] (detailed dilatometric plot is

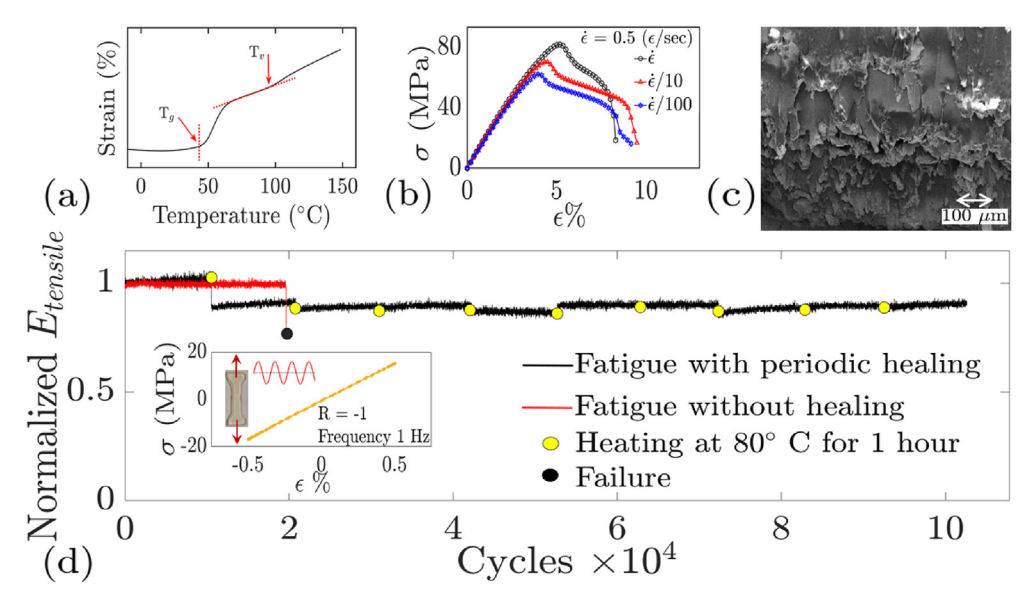


Fig. 2. Reversing fatigue damage in vitrimers by repeated (periodic) doses of healing. (a) Strain measured in a dilatometric experiment with heating rate of ~2.5 K min⁻¹ at stress of ~25 KPa. Glass transition temperature (T_g) and topology freezing transition temperature (T_v) are indicated in the figure. (b) Static tensile testing at room temperature and for three different strain rates. (c) Typical fracture surface image of the failed vitrimer sample with stress-strain curves shown in (b). (d) Fatigue test showing normalized modulus vs. the number of cycles of fatigue loading. Vertical axis is normalized by the initial modulus of the sample, prior to being subjected to fatigue loading. Inset shows the fatigue test scheme (stress-strain loop for one cycle of fatigue loading and the loading parameters). Under these conditions, the vitrimer fails in uniaxial fatigue within ~2 × 10⁴ cycles. However, if the sample is subjected to repeated doses of healing (i.e. heated to ~80 °C for ~1 hour), the fatigue life is extended by at least 5 times (~10⁵ cycles), with no indication of failure. (A colour version of this figure can be viewed online.)

provided in Fig. S6). The onset of this transition is termed as T_v , which is ~79.3 °C for our vitrimer. Differential scanning calorimetry and stress relaxation analysis were also performed; this data (Figs. S7–S8) confirms the T_g and T_v established through dilatometric analysis. Vitrimers were also subjected to shape memory tests, and were observed to recover their shape at elevated temperatures (see Fig. S9) consistent with previous studies [28].

4.2. Static loading analysis

Vitrimer dogbone specimens were subjected to static tensile loading at different strain rates (Fig. 2b). The experimental modulus of the vitrimer is 1.8 ± 0.2 GPa and is insensitive to the loading rate. By contrast, the ultimate tensile strength is dependent on the loading rate and increases from 58 MPa to 78 MPa as strain rate is increased by a factor of 100. This indicates the rate-sensitive viscoelastic nature [29] of the vitrimer, which is further confirmed by fractography analysis. Scanning electron microscopy (SEM) imaging of a typical fracture surface (Fig. 2c) reveals the presence of extensive micro-fibrillation, which indicates ductile failure. This is different when compared with regular epoxy, which is a brittle material and exhibits rapid crack propagation, leaving behind a clean and relatively smooth fracture surface. It should be noted that the 1.8 \pm 0.2 GPa modulus and 67.6 \pm 9.6 MPa ultimate tensile strength that we report for our vitrimer is comparable to commercial state-of-the-art thermosetting epoxies (Table S1, supporting information). In fact, the strain-to-break for the vitrimer (9.08 + 0.62%) is about a factor of two times greater (Table S1) than commercial epoxies. Therefore, unlike thermoplastics which exhibit inferior modulus and strength relative to thermosetting polymers, for our vitrimer chemistry, we do not incur such loss in mechanical properties.

4.3. Fatigue experiment

Next, we investigated the fatigue behavior of the vitrimer. To study fatigue, vitrimer dogbone specimens are subjected to alternating cycling displacement till failure. The modulus is extracted from each load cycle and normalized by the initial modulus at the beginning of the test. This normalized modulus is plotted for each cycle of loading (Fig. 2d). At the point of failure, the normalized modulus drops sharply as the sample fractures. At load ratio, R = -1, sinusoidal test frequency of 1 Hz, and strain amplitude of 0.5% (**inset**, Fig. 2d), the number of cycles to failure for the vitrimer was measured to be ~20,000 cycles. By contrast, when healed after every 10,000 cycles, the epoxy vitrimer shows no indication of failure (even after 100,000 cycles) and this could potentially be enhanced by further repetitions of the healing treatment. The healing involves heating the vitrimer to just above T_v (80 °C) for 1 hour and cooling down to the ambient temperature. After the first healing step, there is a slight drop in modulus. This is to be expected, as heating of the sample would relieve thermal stresses introduced during manufacturing. This is confirmed, since such drop in modulus is not observed after subsequent healing cycles. Thus, we see that by repeated doses of healing treatment, accumulation of fatigue damage in the vitrimer can be periodically reversed. It should be noted that if the healing effectiveness is 100%, then the vitrimer should theoretically exhibit infinite life. In practice, this may not be the case, and future work should involve further testing to establish the limits to which the fatigue life can be extended by this approach.

5. Mechanical testing of vCFRP

The vitrimer developed in this study was used to construct

carbon-fiber prepregs — 8 such prepregs were then stacked and cured to produce vCFRP laminated composites structures (Fig. S10a). Details regarding prepreg and vCFRP fabrication are provided in the Materials and methods Section. vCFRP samples were subjected to flexural load in classic three-point bending (Fig. 3a). Initially the specimen was loaded statically — after the composite reaches peak strength, failure is indicated by stepwise drop in the peak load. indicating progressive failure in individual carbon-fiber plies (Fig. 3b). Maximum bending stress and strain in the sample is computed from beam bending theory. The mean ultimate static strength of vCFRP (σ_u) (maximum tensile stress in the bent sample at failure) is estimated at 448.47 \pm 52.8 MPa. The strength measured was comparable conventional CFRP composites [30] and higher than some of the previously reported vCFRP composites [31]. To analyze fatigue behavior, vCFRP is subjected to fatigue in force-controlled mode, where the maximum stress reached during each cycle is maintained at $\sigma_u/2$. Under these conditions, the vCFRP is subjected to sinusoidal stress cycling (Fig. 3c) till failure. The maximum bending stress and strain in each cycle is used to calculate the bending modulus, which is normalized by the initial modulus to obtain the normalized bending modulus, which is plotted in Fig. 3d vs. the cycle number. The bending modulus of the specimen gradually decreases and eventually drops rapidly at the onset of macroscopic failure. A macroscopic crack (inset, Fig. 3d) is clearly visible across the width of the specimen at the center of the specimen. The gradual reduction in modulus observed in Fig. 3d is indicative of degradation of the vitrimer and the resin-fiber interface.

Next, we subjected vCFRP to the same loading conditions, except that when there was ~10% increase in the maximum displacement over the initial cycle (i.e. with respect to the undamaged vCFRP), the fatigue test was stopped. This compliance increase reflects fatigue damage accumulation in the vCFRP. The vCFRP was healed by heating at ~150 °C for ~1 hour under ~200 kPa pressure. The specimen was then cooled down to the ambient temperature and the fatigue testing was resumed. We observe that after 25 healing cycles (Fig. 3d), the specimen exceeds the lifespan of the baseline vCFRP (i.e. without healing intervention). The normalized bending modulus vs. number of cycles plot further indicates that the modulus drop is reversed after every healing step, with the specimen regaining its original modulus. No flaws are discernible on the sample surface (inset, Fig. 3d) indicating its structural integrity.

SEM imaging of vCFRP specimen was performed to understand the healing mechanism. The sample which was subjected to periodic healing did not exhibit any signs of cracks, matrix damage or matrix-fiber delamination (Fig. 3e), consistent with the morphology (Fig. S10b) of the as-produced vCFRP prior to fatigue loading. However, the sample subjected to the same amount of fatigue loading without healing exhibited clear indication of fibermatrix delamination and fracture in the matrix material (Fig. 3f). As discussed previously, fatigue damage in CFRP composites initiates in the matrix and eventually results in macroscopic fracture and delamination. Hence, the imaging strongly suggest that periodic healing reverses the incipient damage in the matrix, which could otherwise lead to fracture. Since the fiber-matrix interphase is subjected to shear stress during flexural test, interphase damage is also expected to occur in the specimen. It is to be noted that we used a higher healing temperature for the vCFRP (~150 °C in Fig. 3) as compared to the pure vitrimer (~80 °C in Fig. 2). Absence of noticeable delamination suggests that flow of vitrimer material at elevated temperature potentially heals the delamination failure as well. Thus heating vCFRP at elevated temperatures close to the melting point serves dual purpose of healing crosslink rupture as well as delamination. This process, if repeated at periodic intervals can potentially restore vCFRP to virtually pristine condition (Fig. 3g).

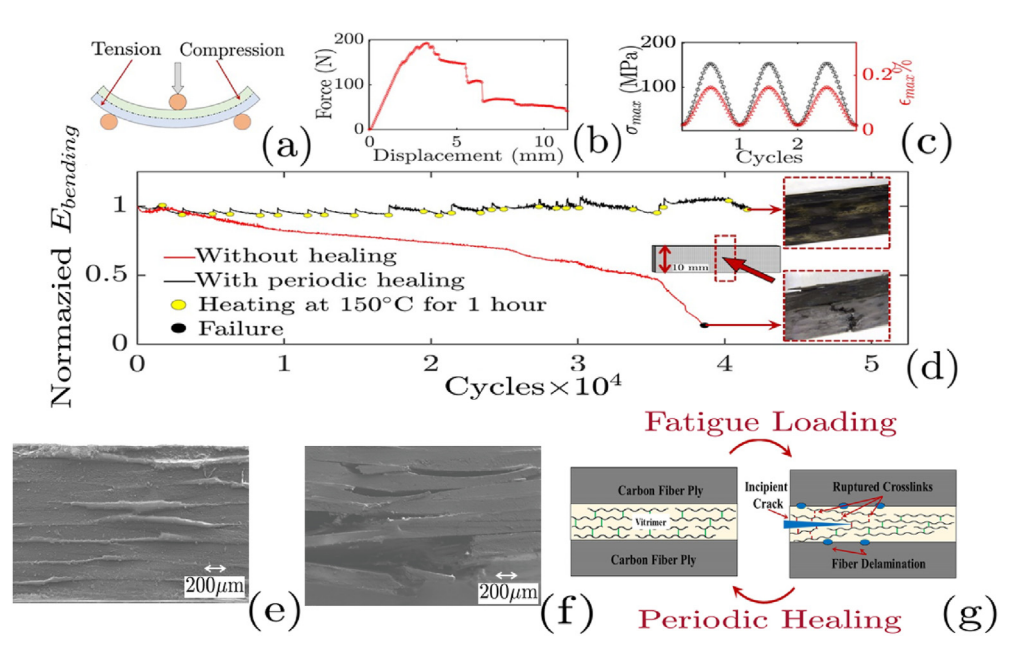


Fig. 3. Reversal of fatigue degradation in vCFRP. (a) Schematic of 3-point bend tests used for vCFRP testing: bending tests subject composites to tension and compression simultaneously. (b) Monotonic bend test for a typical vCFRP specimen, the component reaches a peak followed by a stepwise decline as individual carbon-fiber layers fail. (c) Typical bending stress and strain cycle used in the fatigue experiment; the test is performed in force-control mode. (d) Bending fatigue test for vCFRP indicates that as the load is cycled, the normalized bending modulus drops continuously (red). However, when the vCFRP is heated to ~150 °C for ~1 hour intermittently, the original bending modulus of the specimen is preserved, even as we cycle the vCFRP to high number of loading cycles. Inset optical images shows no apparent cracking of the sample when intermittent healing treatment is applied, while macroscopic cracking is evident in the absence of healing. (e) Scanning electron microscopy (SEM) image of the vCFRP sample which was subjected to periodic healing — no rupture or fiber delamination is observed in this specimen. (f) SEM image of vCFRP sample subjected to the same loading conditions and same number of cycles (without healing) shows clear indication of rupture and fiber-matrix delamination. (g) Schematic explains the process of healing reversal; as vCFRP is subjected to fatigue, vCFRP undergoes crosslink rupture along with fiber-matrix delamination. However, when heated to elevated temperatures, the reversible crosslinks reform and the flow of matrix repairs the small scale fiber-matrix delamination, effectively reversing the fatigue damage. (A colour version of this figure can be viewed online.)

6. Radio frequency heating of vCFRP

So far, we have used conventional oven heating to heal vCFRP. For practical applications, it is important to develop a facile and low-cost method to achieve the uniform volumetric heating of the structure. For this, one can take advantage of the carbon-fibers present in the vitrimer matrix. Carbon materials heat rapidly when exposed to radio frequency (RF) electromagnetic fields. In fact, previous studies have shown [32] that RF fields achieve rapid volumetric heating with higher efficiency as compared to conventional oven heating. Taking advantage of this, we developed a noncontact coplanar capacitor applicator (Fig. S11a) for in situ RF heating of vCFRP. By varying frequency and input power of the RF fields, rapid heating of the vCFRP could be achieved (Fig. S11b); the initial rates reach as high as ~70 °C/sec depending on input RF power. It should be noted that in practical situations, damaged components could be selectively healed by RF heating, while still remaining attached to the structure, without the need to unassemble the system. Such local healing of damaged vCFRP is a key advantage of RF heating, since the RF heating can be applied selectively to locations where the stresses are the greatest, and fatigue damage is most likely to occur.

7. Concluding remarks

In summary, we developed a vitrimeric system that showed comparable modulus, strength and superior ductility in comparison to conventional thermosets. Most importantly, accumulation of fatigue damage in the vitrimer could be "reversed" by periodic healing at temperatures above the topology freezing transition temperature. This vitrimer was used as a matrix to build vCFRP laminates. Fatigue damage to vCFRP could also be reversed by

subjecting the vCFRP to repeated doses of heating treatment. Development of such dynamic polymer composites, that when damaged can be reliably healed, could result in a paradigm shift in how we view the reliability, safety, maintenance and life-cycle cost of structural materials.

Declaration of competing interest

The authors declare that they have no known competing financial interests or personal relationships that could have appeared to influence the work reported in this paper.

Acknowledgments

NK and CRP acknowledge funding support from the US Army/ NASA through the VLRCOE program. NK also acknowledges support from the USA NSF (Award # 2015750) and the John A. Clark and Edward T. Crossan Chair Professorship at the Rensselaer Polytechnic Institute. AV acknowledges support from the University of Washington, Seattle Start-Up funds, and Software for Chemistry & Materials.

Appendix A. Supplementary data

Supplementary data to this article can be found online at https://doi.org/10.1016/j.carbon.2021.10.078.

References

- R. Talreja, C.V. Singh, Damage and Failure of Composite Materials, Cambridge University Press, 2012, ISBN 978-0-521-81942-8.
- [2] R. Huang, M. Huang, X. Li, F. An, N. Koratkar, Z.-Z. Yu, Adv. Mater. 30 (2018), 1707025.

- [3] Composites Market by Fiber Type Global Forecast to 2025. https://www. marketsandmarkets.com/Market-Reports/composite-market-200051282. html. (Accessed 15 June 2020).
- [4] E.T. Thostenson, T.W. Chou, Adv. Mater. 18 (2006) 2837.
- [5] Structural Health Monitoring Market Global Forecast to 2025. https://www. marketsandmarkets.com/Market-Reports/composite-market-200051282. html. (Accessed 15 June 2020).
- [6] P. Alam, D. Mamalis, C. Robert, C. Floreani, C.M.Ó. Brádaigh, Compos. B Eng. 166 (2019) 555-579.
- [7] S. Riaz, S.-J. Park, Macromol. Res. 28 (2020) 1116.
- [8] S. Riaz, S.-J. Park, Compos. Appl. Sci. Manuf. 146 (2021), 106419.
- [9] A. Zandiatashbar, C.R. Picu, N. Koratkar *Small* 8 (2012) 1676.
- [10] M. Rafiee, J. Rafiee, Z. Wang, H. Song, Z.-Z. Yu, N. Koratkar, ACS Nano 3 (2009) 3884
- [11] T.H. Hsieh, A.J. Kinloch, K. Masania, A.C. Taylor, S. Sprenger, Polymer 51 (2010) 6284.
- [12] M. Rafiee, J. Rafiee, F. Yavari, N. Koratkar, J. Nanoparticle Res. 13 (2011) 733.
 [13] I. Srivastava, R.J. Mehta, Z.-Z. Yu, L. Schadler, N. Koratkar, Appl. Phys. Lett. 98 (2011) 063102
- [14] S.R. White, N.R. Sottos, P.H. Geubelle, J.S. Moore, M.R. Kessler, S.R. Sriram, E.N. Brown, S. Viswanathan, Nature 409 (2001) 794.
- [15] V.K. Thakur, M.R. Kessler, Polymer 69 (2015) 369.
- [16] A.K. Jain, A.K. Nagpal, R. Singhal, N.K. Gupta, J. Appl. Polym. Sci. 78 (2000) 2089

- [17] D. Montarnal, M. Capelot, F. Tournilhac, L. Leibler, Science 334 (2011) 965.
- [18] N. Zheng, Y. Xu, Q. Zhao, T. Xie, Chem. Rev. 121 (2021) 1716.
- [19] A.M. Hubbard, Y. Ren, D. Konkolewicz, A. Sarvestani, C.R. Picu, G.S. Kedziora, A. Roy, V. Varshney, D. Nepal, ACS Applied Polymer Materials 3 (2021) 1756.
- [20] N.J. Van Zee, R. Nicolay, Prog. Polym. Sci. 104 (2020), 101233.
- [21] S. Ciarella, R.A. Biezemans, L.M. Janssen, Proc. Natl. Acad. Sci. Unit. States Am. 116 (2019), 25013.
- [22] V. Varshney, S.S. Patnaik, A.K. Roy, B.L. Farmer, Macromolecules 41 (2008) 6837.
- [23] P.H. Lin, R. Khare, Macromolecules 42 (2009) 4319.
- [24] A. Vashisth, C. Ashraf, W. Zhang, C.E. Bakis, A.C. Van Duin, J. Phys. Chem. 122 (2018) 6633.
- [25] W. Zhang, A.C. Van Duin, J. Phys. Chem. B 122 (2018) 4083.
- [26] R.A. Miron, K.A. Fichthorn, J. Chem. Phys. 119 (2003) 6210.
- [27] A. Vashisth, C. Ashraf, C.E. Bakis, A.C. Van Duin, Polymer 158 (2018) 354.
 [28] Z. Pei, Y. Yang, Q. Chen, Y. Wei, Y. Ji, Adv. Mater. 28 (2016) 156.
- [29] W. Denissen, M. Droesbeke, R. Nicolaÿ, L. Leibler, J.M. Winne, F.E. Du Prez, Nat. Commun. 8 (2017) 14857.
- [30] Kamble Mithil, Aniruddha Singh Lakhnot, Stephen F. Bartolucci, Andrew G. Littlefield, Catalin R. Picu, Nikhil Koratkar, Carbon 17 (2020) 220–224.
- [31] Luxia Yu, Chengpu Zhu, XiaoHao Sun, Jacob Salter, HengAn Wu, Yinghua Jin,
- Wei Zhang, Rong Long, ACS Applied Polymer Materials 1 (9) (2019) 2535.

 [32] N. Patil, X. Zhao, N.K. Mishra, M.A. Saed, M. Radovic, M.J. Green, ACS Appl. Mater. Interfaces 11 (2019) 46132.